MIT Open Access Articles

Steady States and Dynamics of Urokinase-Mediated Plasmin Activation In Silico and In Vitro

Massachusetts Institute of Technology

Steady States and Dynamics of Urokinase-Mediated Plasmin Activation In Silico and In Vitro

Lakshmi Venkatraman,[†¶‡] Huipeng Li,[†] C. Forbes Dewey, Jr.,[†‖] Jacob K. White,[†**] Sourav S. Bhowmick,[†¶] Hanry Yu,[†‡§††*] and Lisa Tucker-Kellogg[†‡*]

[†]Singapore-MIT Alliance, [‡]Mechanobiology Institute, and [§]Department of Physiology, National University of Singapore, Singapore; [¶]School of Computer Engineering, Nanyang Technological University, Singapore; [‖]Department of Mechanical Engineering and [**]Department of Electrical Engineering and Computer Science, Massachusetts Institute of Technology, Cambridge, Massachusetts; and [††]Institute of Bioengineering and Nanotechnology, A*STAR, Singapore

ABSTRACT Plasmin (PLS) and urokinase-type plasminogen activator (UPA) are ubiquitous proteases that regulate the extracellular environment. Although they are secreted in inactive forms, they can activate each other through proteolytic cleavage. This mutual interplay creates the potential for complex dynamics, which we investigated using mathematical modeling and in vitro experiments. We constructed ordinary differential equations to model the conversion of precursor plasminogen into active PLS, and precursor urokinase (scUPA) into active urokinase (tcUPA). Although neither PLS nor UPA exhibits allosteric cooperativity, modeling showed that cooperativity occurred at the system level because of substrate competition. Computational simulations and bifurcation analysis predicted that the system would be bistable over a range of parameters for cooperativity and positive feedback. Cell-free experiments with recombinant proteins tested key predictions of the model. PLS activation in response to scUPA stimulus was found to be cooperative in vitro. Finally, bistability was demonstrated in vitro by the presence of two significantly different steady-state levels of PLS activation for the same levels of stimulus. We conclude that ultrasensitive, bistable activation of UPA-PLS is possible in the presence of substrate competition. An ultrasensitive threshold for activation of PLS and UPA would have ramifications for normal and disease processes, including angiogenesis, metastasis, wound healing, and fibrosis.

INTRODUCTION

Plasmin (PLS) is a serine protease that is best known for its role in digesting blood clots, but it has many substrates and far-reaching physiological functions in hemostasis (1), angiogenesis (2), wound healing (3,4), and cell motility, including migration and metastasis (5). For example, it activates matrix metalloproteases (MMPs; e.g., MMP1, MMP3, and MMP13 (6,7)) and regulates growth factors (e.g., VEGF (8), HGF (9), and TGF-β1 (10)). Spatiotemporal control of PLS availability occurs through localized activation of the inactive precursor plasminogen (PLG), which is widely available through circulation. The cleavage of PLG to make active PLS occurs at the Arg^{561}-Val^{562} bond, caused by tissue plasminogen activator (tPA) or urokinase-type plasminogen activator (UPA). tPA influences PLS activation mainly in the connective tissues, whereas UPA plays a more important role in the extracellular matrix (ECM) of tissues (11). Regulation of PLS activity is also controlled by the specific inhibitors α-2-macroglobulin (A2M) or α-2-anti-PLS (A2P) (12).

Protease activation can be categorized according to regulatory motifs such as auto-activation (Fig. 1 A), in which an active protease X cleaves its inactive precursor form. An alternative manner of activation (Fig. 1 B) operates via regulation of an intermediate regulatory enzyme (Y), which also

has active and precursor forms. This type of positive feedback is seen in pathways such as caspase activation (13,14), MMP activation (15), and blood clotting (16). Fig. 1 C displays a variant in which the precursor form of Y has some low level of catalytic activity, less than the activated form but not entirely inactive. Urokinase exhibits a low level of zymogen activity, and the final motif (Fig. 1 C) describes the biochemical relationship between PLS and UPA.

The signaling dynamics of positive feedback loops have been extensively modeled (17,18), most commonly for kinase cascades (19–21). Computational modeling is particularly useful for elucidating the bifurcations, qualitative changes in pathway behavior, and emergent behaviors that arise in a complex system (18–22). Bistability, or the presence of two stable steady states, has been shown to be crucial for making robust yes-or-no decisions in cell cycle and apoptosis (23). Eissing et al. (24) explored the requirements for bistability in a feedback loop with two proteases. Substrate competition has been found to influence bistability for kinases (25), but has not yet been modeled for proteases. Because proteases (e.g., caspases) typically have many competing substrates (26) and sometimes have initial zymogen activity (27), the effects of substrate competition and zymogen activity might be important considerations for future system-level modeling.

In this work, we modeled the dynamics of UPA-mediated PLS activation and performed biochemical experiments to test key predictions of the model. The model predicts that UPA-PLS
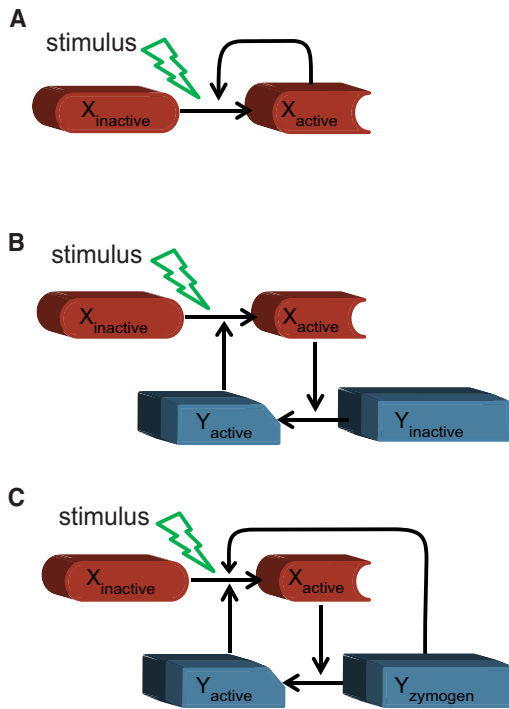
FIGURE 1 Motifs of protease activation. (*A*) Simplistic model of protease auto-activation. An external stimulus may initiate activation of the protease. (*B*) A positive feedback loop between two proteases. Once the initiator protease (X_{active}) is activated, it activates a downstream inactive protease ($Y_{inactive}$ to Y_{active}), which can then provide feedback on $X_{inactive}$ to make more X_{active}. (*C*) The same motif as in *B* except the precursor of the inactive initiator protease ($Y_{zymogen}$) has some endogenous activity.

activation will be bistable in the presence of positive feedback and cooperativity. An extended model predicts that PLS activation will exhibit significant cooperativity in the presence of substrate competition. We performed in vitro experiments to test the cooperativity of PLS activation, and to measure the bi- or monostability of the PLS steady-state convergence. The results are interpreted in the context of physiological systems in which UPA and PLS are known to function.

MATERIALS AND METHODS

Computational methods

We simulated ordinary differential equations (ODEs) using the ODE15s stiff solver of MATLAB (The MathWorks, Natick, MA; http://www.mathworks.com). For simulations with random initial conditions, we generated 100 initial concentrations for all species uniformly at random between 1 nM and 0.1 μM using Latin hypercube sampling. Each of these conditions was simulated with the use of the ODE solver until a steady state was obtained.

We tested for bistability using simulation-based analysis of "going-up" and "coming-down" transitions as described previously (13,28). For the "going-up" curves (*red lines*), a specified parameter of the model was perturbed over a range of values. For each value of the parameter, the system was initialized in an inactive state and then simulated until a steady state was achieved (within 50,000 steps). For the "coming-down" simulations

(*blue curves*), the same range of parameter values was tested, except that for each "coming-down" test, the system was initialized in the higher steady state. For parameter values that caused monostable behavior of the system, the steady-state outcome did not depend on how the system was initialized. However, bistability was demonstrated if the "going-up" and "coming-down" simulations showed a range of parameter values for which the system achieved two different steady states, depending on the initialization.

We obtained bifurcation diagrams using XPPAUT (http://www.math.pitt.edu/~bard/xpp/xpp.html). For the robustness analysis (see Fig. 6 *B*), we generated 100 random parameter vectors using Latin-hypercube sampling (13,14) with $\pm 20\%$ to $\pm 50\%$ perturbation of the parameters from the nominal values. We then calculated the number of parameter sets that were capable of bistability using the "going-up" and "coming-down" simulations. For Fig. 6 *C*, the parameter of interest was fixed while all other parameters were randomly perturbed by $\pm 20\%$ or $\pm 50\%$ from the nominal values. A parameter set is considered bistable if the difference between the high and low steady states of PLS is >0.03 μM. Note that 0.007 μM and 0.0375 μM are the two steady states of PLS obtained from the model shown in Table 2 with substrate competition and cooperativity index (ci) $= 1$.

The Hill coefficient (n_H) was calculated with the use of the statistical software GraphPad prism (Graphpad Software; San Diego, CA).

Experimental methods

All solutions were prepared in Tris buffer (0.05 M Tris-HCL, 0.10 M NaC1, 0.01% Tween 80, pH 7.4). The chromogenic substrate of PLS, S2251 (0.4 mM), with chemical formula H-D-Val-Leu-Lys-pNA.2HCl, was purchased from Chromogenix (Milano, Italy). In the presence of PLS, the following reaction occurs, releasing pNA:

$$\text{H-D-Val-Leu-Lys-pNA} + \text{PLS} \rightarrow \text{H-D-Val-Leu-Lys-OH}$$
$$+ \text{pNA}.$$
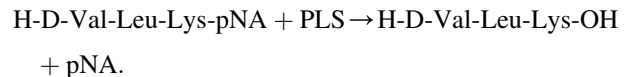
The color intensity of pNA can be measured at an O.D. of 405 nm. For the test of cooperativity, we used variable amounts of scUPA (0.1–6 nM; American Diagnostica, Greenwich, CT) along with a nonvariable initial concentration of 1 μM PLG (Glu-PLG; Merck, Darmstadt, Germany). The changing color intensity of S2251 (absorbance), which is a direct measure of PLS activity, was measured at O.D. $= 405$ nm with a TecanM200 microplate reader. During the experiments, scUPA and PLG were added manually every 15 min at rates of 50 pM/min and 1 nM/min, respectively (in volumes of ~0.2 μL) to simulate the turnover that would occur in a natural system. The total volume of the reaction solution was 200 μL. No S2251 was added. The "going-up" experiments were initiated with PLS (Sigma, St. Louis, MO) and PLG concentrations in the ratio 60% PLG/40%PLS (0.6 μM PLG, 0.4 μM PLS). Various initial concentrations of scUPA were added, and PLS steady state was measured. For the "coming-down" experiments, the ratio was reversed (0.4 μM PLG, 0.6 μM PLS) and the same series of scUPA levels was used.

RESULTS

Construction of the model

UPA is a trypsin-like serine protease that is initially secreted as a single intact chain, scUPA (29–31). The intrinsic enzymatic activity of scUPA is used to initiate the cleavage of inactive PLG (No. 1 in Table 1 and Fig. 2). Cleavage of PLG at the Arg[561]-Val[562] bond releases the active serine protease, PLS. Active PLS can cleave scUPA at the Lys[158]-Ile[159] backbone, releasing a two-chain form (tcUPA;
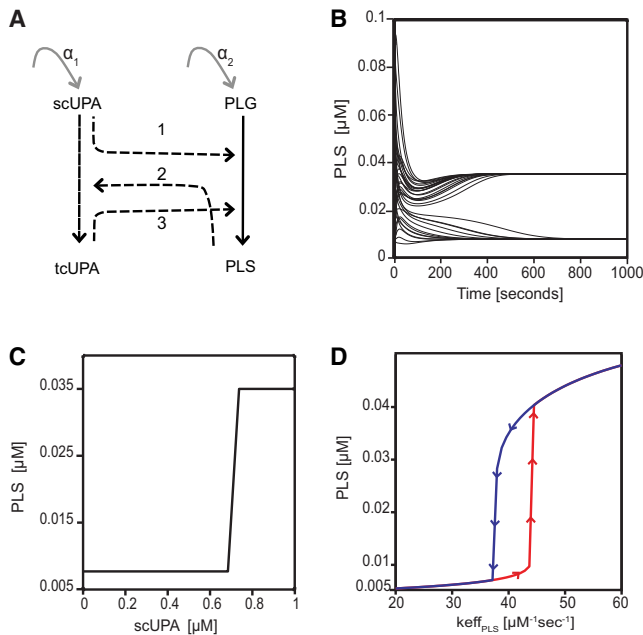
FIGURE 2   Model of UPA-mediated PLS activation. (*A*) The initiator precursor protease scUPA activates PLG to form PLS (*arrow 1*). PLS cleaves scUPA to produce the completely active tcUPA form (*arrow 2*), which can then provide feedback on PLG to make more PLS (*arrow 3*). Enzymatic reactions (*dashed arrows*) catalyze transitions (*solid arrows*) between substrate and product. (*B*) Convergence of PLS concentration over time, after the model is initialized with random concentrations of all the species. (*C*) A transition of the PLS steady state that is dependent on the initial concentration of scUPA. (*D*) "Going-up" (*red line*) and "coming-down" (*blue line*) simulations obtained using different values of $keff_{PLS}$ while measuring PLS steady-state levels. Arrows follow the transition of PLS concentrations from one steady state to another with changing parameter values. The simulations were done using the parameter values in Table 2 with $ci = 2$.

No. 2 in Table 1 and Fig. 2) in which the two chains are linked by a disulphide bridge. tcUPA has 12-fold higher enzymatic activity than scUPA for cleaving PLG to PLS (No. 3 in Table 1 and Fig. 2 *A*). The interdependent proteolytic activation of tcUPA and PLS is consistent with the motif of Fig. 1 *C*.

The interactions between UPA and PLS (Fig. 2 *A*) were expressed as ODEs (see Table S1 in the Supporting Material) for the concentration change of each species with respect to time. Enzyme kinetics were approximated with linear terms using the catalytic efficiency keff = $kcat/k_M$. The use of linear terms, rather than more complex Michaelis-Menten kinetics, was chosen because the k_M parameters are much greater than the substrate concentrations (31–33). Table 2 shows key terms of the equations, numbered to correspond with the arrows in Fig. 2 *A*. We used constant rates to model production of the precursor forms (scUPA and PLG) and first-order degradation rates for all species, with the rate constants given in Table 2. Production and degradation are particularly important in this model because proteolysis reactions are irreversible and, in the absence of

turnover, the steady state of the system would tend toward a trivial, nonphysiological situation of total cleavage. Substrate competition can create cooperativity in enzyme action, apart from the traditional mode of allosteric cooperativity (25). Because PLS has many substrates, we allowed it to have a cooperative effect on UPA with an empirical Hill coefficient ($ci > 1$) in the equation for PLS enzyme kinetics. In subsequent analysis, the case of $ci = 1$ will also be explored. Most of the other parameters have values from experimental measurements obtained in previous studies (Table 2).

Model simulation analysis

The model ODEs were simulated with randomly generated initial concentrations between 1e-3 μM and 0.1 μM. The steady states of the model show that PLS converges over time to two different concentrations (0.007 μM or 0.035 μM; Fig. 2 *B*). The presence of more than one steady state indicates that complex dynamics is an emergent behavior of the system.

For subsequent plots of model behavior, instead of displaying a horizontal time axis, we define the output of each simulation to be simply the final PLS concentration (at steady state). Fig. 2 *C* shows a projection of many time-series simulations onto a single curve, showing that the transition between the two steady states of PLS can be triggered by changing the initial concentration of the initiator protease scUPA. This abrupt increase in the PLS steady state upon a change in the initial scUPA concentration demonstrates that the model is ultrasensitive, meaning that small perturbations of the parameters can cause significant changes in model output (34). For concentrations of scUPA < 0.7 μM, PLS is maintained at the lower steady state, and for concentrations of scUPA above this threshold value, PLS levels increase abruptly to a higher steady state. One way to understand this behavior is to consider that higher initial concentrations of scUPA can provide greater amounts of PLS and cause more activation of tcUPA. Because tcUPA has a higher catalytic efficiency than scUPA, an increase in PLS generation occurs via the positive feedback loop. In contrast, lower scUPA concentrations would not create PLS quickly enough to overcome the background degradation, and would not increase tcUPA levels enough to exploit the positive feedback loop. These results indicate that, depending on the initial concentrations of model species, the system is ultrasensitive. Ultrasensitive systems have been shown to be capable of bistability (34), and we checked for the presence of bistability in the current system by varying parameter values and following the steady-state behavior.

We simulated PLS steady-state levels using a "going-up" and "coming-down" approach (28). The values of $keff_{PLS}$ (catalytic efficiency of PLS), would control the amount of tcUPA present in the system, and also indirectly regulate the effect of tcUPA on PLG to produce more PLS. $keff_{PLS}$

was varied along two directions ("going-up" and "coming-down") and the amounts of PLS in the final steady states (calculated to 50,000 steps) were plotted (Fig. 2 *D*). A bistable phenomenon was noticed during this simulation. Increasing values of keff$_{PLS}$ were seen to gradually increase the stable steady-state levels of PLS until keff$_{PLS}$ reached the parameter value of $>40 \ \mu M^{-1}s^{-1}$ (Fig. 2 *D*, *red curve*, "going-up"). At this threshold of keff$_{PLS}$, there was enough tcUPA in the system to propel PLS levels to a higher stable steady state. Decreasing the keff$_{PLS}$ parameter from this point did not make PLS drop down into the lower steady state at the same threshold value. PLS was maintained at a high level for a broader range of parameter values until keff$_{PLS}$ reached a second threshold of $< 33.5 \ \mu M^{-1}s^{-1}$, and only then did PLS steady-state levels drop down. The region between these two threshold values of keff$_{PLS}$ is the bistable region; depending on the initial conditions, PLS could achieve steady state at either a higher or lower level. The phenomenon of remembering an earlier state (or an earlier concentration level), even when the stimulus is removed, is called hysteresis.

Bistability in a system has been shown to depend on positive feedback and cooperativity (35). We assessed the significance of positive feedback and cooperativity on model bistability by modifying these parameters. We refer to the rate at which tcUPA converts PLG into PLS as the positive feedback rate, keff$_{pos}$. The parameter ci is the Hill coefficient of PLS and represents the cooperativity in PLS action due to substrate competition effects. In the absence of positive feedback (keff$_{pos} = 0 \ \mu M^{-1}s^{-1}$), increasing ci creates a monostable PLS concentration at the lower steady state because there is not enough conversion of inactive PLG to PLS (Fig. 3 *A*). When the strength of positive feedback, keff$_{pos}$, is increased to $0.1 \ \mu M^{-1}s^{-1}$, the positive feedback causes increased PLS activation, but PLS is still maintained at a monostable state. When the positive feedback signal, keff$_{pos}$, increases to 0.5, 1, 2, or $3 \ \mu M^{-1}s^{-1}$, PLS exhibits two steady states. The transition between monostability and bistability along the ci variable is shown by black dots, which denote the values of ci at which saddle node (SN) bifurcations occur for a given value of keff$_{pos}$. When a value of ci is chosen between these SN bifurcation points (SNI and SN2 on the curve for keff$_{pos} = 3 \ \mu M^{-1}s^{-1}$), the resulting system has two stable fixed points and one unstable fixed point between them. The gray arrow in Fig. 3 *A* indicates the evolution of PLS steady state with increasing keff$_{pos}$ values. Increasing the positive feedback strength facilitates bistability in the system and also increases the area of bistability, as illustrated by the two-parameter bifurcation diagram (*gray region* in Fig. 3 *B*) in which the parameters keff$_{pos}$ and ci are perturbed simultaneously. The shaded region indicates bistability, and the models in the other nonshaded portions are monostable. Fig. 3 *B* indicates that increasing keff$_{pos}$ yields a wider range of ci values with bistability. The two solid lines bordering the shaded cusp
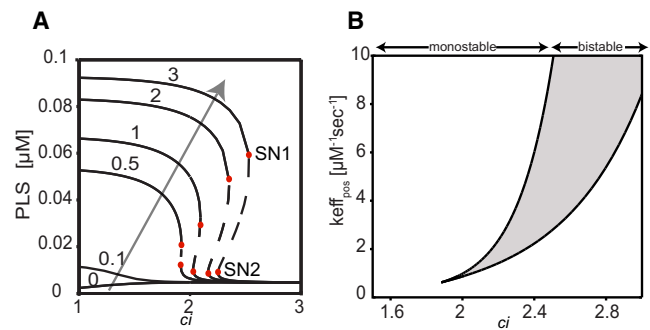
FIGURE 3 Dependence of bistability on the parameters for positive feedback and cooperativity. (*A*) Bifurcation diagram of PLS bistability over parameter ci for different values of the positive feedback parameter, keff$_{pos}$ (0, 0.1, 0.5, 1, 2, and $3 \ \mu M^{-1}s^{-1}$; labeled above each curve). Dark lines are the stable steady states; dashed lines are unstable steady states. SN1 and SN2 are the SN bifurcations shown as circular dots. The light gray line depicts the shift in PLS steady-state levels with a progressive increase in keff$_{pos}$ values. (*B*) A two-parameter bifurcation diagram between keff$_{pos}$ and ci values, with PLS steady states determining bistability. The region within the cusp (i.e., the *gray-shaded area*) represents the bistable PLS levels, and the remaining area shows the monostable PLS levels.

represent SN bifurcations between monostability and bistability.

Although cooperativity and positive feedback are both favorable toward bistability, they can also destroy bistability if they are not balanced with respect to each other. Even as increased values of keff$_{pos}$ cause an increased area of bistability, they require an increase in ci (rightward shift in Fig. 3, *A* and *B*) to maintain the bistability. Bistability is possible when the increased production of PLS (due to higher keff$_{pos}$) is counterbalanced by increased production of tcUPA (due to higher ci). Positive feedback between tcUPA and PLS has been described previously (33), and the source of positive feedback is obvious from the reactions of mutual activation. Cooperativity has not been reported for PLS or UPA; therefore, we explored the possibility that cooperativity arises from substrate competition.

Effect of substrate cooperativity on model dynamics

We tested whether adding an explicit additional substrate of PLS could createl cooperativity and reproduce the effect of having a Hill coefficient $ci > 1$ in the PLS kinetic equation. Enzyme cooperativity occurs when increasing the concentration of an enzyme causes a nonlinear (greater than additive) increase in activity (36). Cooperativity between multiple phosphorylation sites has been shown to be responsible for bistability in MAPK cascades (20). Another form of kinase-phosphatase cooperativity was discussed by Kim and Ferrell (25), who showed that increasing the substrates of the cell cycle kinase cdk1 caused an intrinsic cooperativity in the action of cdk1 and wee1. This cooperativity in turn could cause the bistable switching of their system.

PLS also has multiple substrates, so we sought to determine whether the activity of PLS on scUPA is cooperative in the presence of competing substrates. We constructed an extended model with a new PLS substrate, X (Fig. 4 A). For the hypothetical analogy between the model and the reality in vivo, species X corresponds to one or more physiological substrates with high affinity for PLS. (For validation experiments in vitro, as described in the following section, an exogenous high-affinity reagent (S2251) will be introduced in the role of species X.)

In the extended model, substrate X can bind PLS and form a complex (X.PLS). This complex can dissociate or undergo a catalytic reaction in which PLS consumes X and reverts to the unbound state. All simulations of the extended model were performed with no cooperativity built in explicitly, i.e., $c_i = 1$. Additional parameters and values are given in Table 2. To analyze the extended model, the PLS parameter $keff_{PLS}$ was perturbed. The steady-state endpoints for PLS were computed, and these endpoints were compiled into a "going-up"/"coming-down" plot as de-

TABLE 1 List of reaction equations

1. $scupa + plg \xrightarrow{keff_{zymogen}} pls + scupa$	8. $pls + X \underset{k_{-1}}{\overset{k_1}{\rightleftharpoons}} Xpls$
2. $pls + scupa \xrightarrow{keff_{pls}} tcupa + pls$	9. $Xpls \xrightarrow{k_2} pls$
3. $tcupa + plg \xrightarrow{keff_{pos}} pls + tcupa$	10. $X \xrightarrow{\mu_2}$
4. $scupa \xrightarrow{\mu_1}$	11. $Xpls \xrightarrow{\mu_2}$
5. $plg \xrightarrow{\mu_2}$	12. $\xrightarrow{\alpha_1} scupa$
6. $pls \xrightarrow{\mu_1}$	13. $\xrightarrow{\alpha_2} plg$
7. $tcupa \xrightarrow{\mu_1}$	14. $\xrightarrow{\alpha_3} X$

scribed in Materials and Methods. The results show that even if $c_i = 1$, PLS can be bistable (Fig. 4 B). In fact, the area of bistability in this extended model is greater than that in the model with $c_i = 2$ and no substrate competition (compare with a similar plot from Fig. 2 C). Adding substrates into the model has an overall effect similar to that obtained by increasing the c_i, as in Fig. 3 A. Added substrates sequester PLS away from the scUPA, unless PLS can consume the competing substrate more quickly than the turnover rate. At a threshold level of $keff_{PLS}$, PLS can finally overcome the competition and the system can move into a higher steady state. Substrate competition creates cooperativity because a small increase in PLS activity tips the balance toward consuming the substrate, releases some PLS from sequestration, and causes a greater-than-additive effect on scUPA.

We next examine the affinity of the competing substrate X, because the relative affinity of X and scUPA for PLS
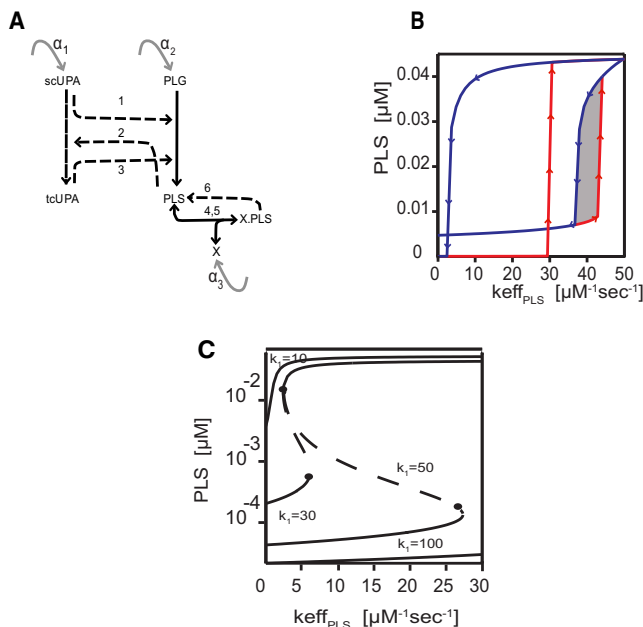
FIGURE 4 Substrate competition and bistability. (*A*) Model extended by addition of substrate X, which binds reversibly to PLS (*arrows 4 and 5*). After forming a complex of PLS and substrate X (X.PLS), PLS can cleave X and return to the system unbound (*arrow 6*), whereas the cleaved substrate is degraded/consumed. Catalytic reactions are indicated with dashed lines. (*B*) The effect of substrate competition on the area of PLS steady-state bistability. The shaded gray area of bistability on the right side of the plot pertains to the original model with $c_i = 2$ and no substrate competition. The broader (*unshaded*) area of bistability on the left pertains to the extended model with one competing substrate and no explicit cooperativity ($c_i = 1$). Red indicates "going–up" and blue indicates "coming–down", with changing values of parameter $keff_{PLS}$. (*C*) The dependence of bistability on k_1, the affinity of the competing substrate toward PLS steady state. Dark lines are stable steady states, and dashed lines are unstable steady states. Black dots indicate SN bifurcations.

TABLE 2 Reaction equations and parameters of the computational model

Reaction equation terms	Parameters	References
$v_1 = keff_{zymogen} \times [scUPA] \times [PLG]$	$keff_{zymogen} = 0.035\ \mu M^{-1}s^{-1}$	(31)
$v_2 = keff_{PLS} \times [scUPA] \times [PLS]^{ci}$	$keff_{PLS} = 40\ \mu M^{-1}s^{-1}$	(31)
$v_3 = keff_{pos} \times [tcUPA] \times [PLG]$	$keff_{pos} = 0.9\ \mu M^{-1}s^{-1}$	(31)
$v_4 = k_1 \times [PLS] \times [X]$	$k_1 = 50\ \mu M^{-1}s^{-1}$	(48)
$v_5 = k_{-1} \times [XPLS]$	$k_{-1} = 0.016\ s^{-1}$	(48)
$v_6 = k_2 \times [XPLS]$	$k_2 = 0.02\ s^{-1}$	variable
ci	2 or 1	variable
μ_1	$\mu_1 = 0.084\ s^{-1}$	(45,49)
μ_2	$\mu_2 = 0.032\ s^{-1}$	(50,51)
μ_3	$\mu_3 = 0.0032\ s^{-1}$	(50,51)
α_1	$\alpha_1 = 0.0032\ s^{-1}$	(45,52)
α_2	$\alpha_2 = 0.01\ s^{-1}$	(45,52)
α_3	$\alpha_3 = 0.01\ s^{-1}$	variable

Velocity terms v_1–v_6 correspond to the reaction arrows numbered 1–6 in Figs. 2 and 4. Complete differential equations appear in Table S1. Parameters listed as variable were not assigned parameter values from the literature. Initial concentrations of the species in μM: scUPA, PLG, PLS, tcUPA, X, and XPLS = 0.002, 0.01, 0, 0, 0.2, and 0, respectively.

can regulate the sequestration effect. As shown in Fig. 4 C, PLS steady-state values were simulated with different values of k_1 (the rate of substrate X binding to PLS) but with $ci = 1$ maintained in all cases. For low substrate binding ($k_1 = 10$ $\mu M^{-1} s^{-1}$), PLS exhibits a monostable high steady state because there is no high-affinity substrate to sequester the enzyme. With increasing values of k_1 (30 $\mu M^{-1} s^{-1}$, 50 $\mu M^{-1} s^{-1}$; Fig. 4 C), i.e., in presence of higher-affinity substrates, sequestration of PLS by the substrates increases, as evidenced by the increased retention of PLS in the lower steady state for higher values of keff$_{pls}$. For subsequent increased k_1 values, higher values of PLS enzymatic activity are needed before PLS can make the transition to the higher steady state. However, very high-affinity substrates (e.g., with $k_1 = 100$ $\mu M^{-1} s^{-1}$) keep PLS in a monostable lower steady state. This shows that a high-affinity substrate can sequester PLS and prevent it from triggering the transition to a high steady state. For intermediate values of k_1, PLS can be bistable, with the area of bistability increasing as k_1 increases. This shows that substrate competition is capable of producing enough nonlinearity in the PLS kinetics to generate two stable steady states for the system.

Experimental validation of model-based predictions

We experimentally tested whether ultrasensitivity and bistability could be observed in UPA-mediated PLG activation using a cell-free experimental system. Different concentrations of scUPA were added to a constant 1 nM of PLG and S2251 chromogenic substrate (0.4 mM) to detect PLS activity. S2251 served both to monitor the activity of PLS and as a high-affinity substrate for PLS, because S2251 would compete with scUPA for the active site of PLS. PLS activity was monitored over time until a steady state was reached (in ~4 h; Fig. S2). During the experiment, constant exogenous additions of small quantities of PLG and scUPA were provided to reproduce constant production. PLS steady-state curves (Fig. 5 A) in response to varying initial concentrations of scUPA yielded a sigmoidal curve (Hill coefficient $n_H = 1.3$), demonstrating cooperative behavior.
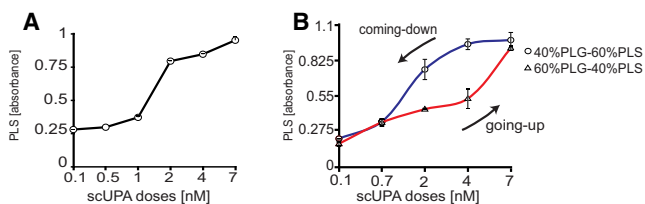

FIGURE 5 Experimental tests of ultrasensitivity and bistability. (A) PLS activity measured experimentally after different doses of recombinant scUPA in the presence of substrate competition (chromogenic substrate) and weak external production of precursor proteins. (B) PLS steady states for different initial levels of PLS/PLG activation and different doses of scUPA.

The above results, however, do not indicate bistability. The presence of hysteresis would be more affirmative evidence for bistability of the system (34). For hysteresis, the system must exhibit two different steady states depending on the initial concentrations, without requiring any alteration of the rates (including synthesis/degradation). The experiment to test hysteresis was performed with two different initial states: one with a low initial concentration of PLS and one with higher PLS. To set up the state with low PLS, we used a 60:40 ratio of PLG/PLS, and for the state with high PLS, we used a 40:60 ratio of PLG/PLS. In other words, the same amount of total PLG/PLS protein was provided to both cases and only the initial extent of PLG/PLS activation was varied. Each of these states was then given a variable dose of scUPA (1–7 nM) and PLS activity was followed. Note that the S2251 chromogenic substrate was present to enable detection of PLS activity, but it also served as a potential source of substrate competition. For very low amounts of added scUPA, PLS reached the same steady-state level, with minimal activation, irrespective of whether we started from a high (60:40 ratio) or low (40:60 ratio) PLS initial condition. Similarly, for very high amounts of initial scUPA, PLS reached high steady-state levels irrespective of the initial PLG/PLS ratio. However, for an intermediate concentration between 2 nM and 7 nM of initial scUPA levels, PLS converged to two different steady states depending on its initial concentration (Fig. 5 B). For example, at 2 nM of scUPA stimulus, the experimental setup of high PLG (i.e., 60:40 ratio) had low PLS and remained at the lower steady state, whereas for the same initial stimulus of 2nM scUPA, the experimental setup with higher initial PLS (i.e., 40:60 ratio) achieved the high steady state of activation. The cell-free experiments therefore demonstrate that scUPA-mediated activation of PLS from PLG is bistable.

Sensitivity and robustness analyses

The parameters used for model construction (Fig. 4 A) were assembled from different literature sources and therefore should be considered highly approximate. Fig. 6 A is a two-parameter bifurcation diagram that characterizes the robustness of model bistability with respect to variation in the parameters k_1 (substrate binding) and keff$_{PLS}$ (PLS efficiency). The shaded region inside the cusp represents models with bistability, and the boundary lines represent SN bifurcations. We next generated 100 random parameter sets with $\pm 20\%$ to $\pm 50\%$ variation from the 13 nominal parameters in Table 2 (see Materials and Methods). For each parameter vector, bistability was tested with the "going-up" and "coming-down" simulations (28). Fig. 6 B shows the percent bistability, i.e., the proportion of parameter sets that are capable of bistability when all parameters are varied. There is only a threefold decrease in percent bistability when parameters are varied from $\pm 20\%$ to $\pm 40\%$ of the nominal
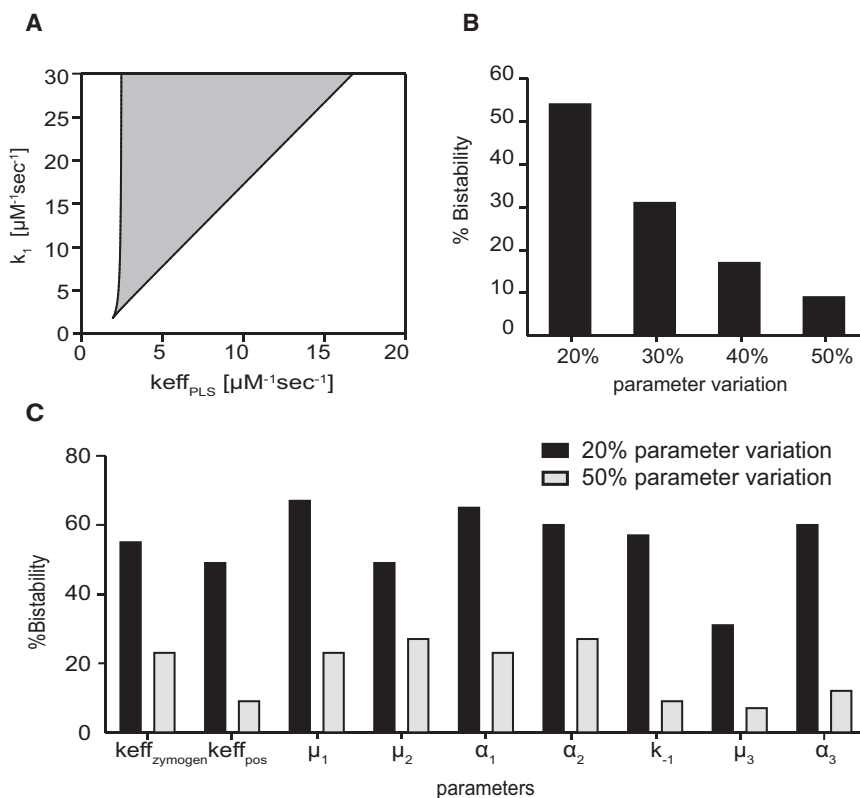
FIGURE 6 Robustness analyses. (*A*) A two-parameter bifurcation diagram with respect to parameters k_1 (substrate affinity) and $keff_{PLS}$ (PLS efficiency) depicts the area of bistability (i.e., the shaded portion inside the cusp). (*B*) Using parameter vectors generated with $\pm 20\%$ to $\pm 50\%$ random variation from the nominal parameters, the percent of models retaining bistability was calculated using $keff_{PLS}$ as the bifurcation parameter. (*C*) Percent bistability when each parameter is perturbed individually (see "Computational methods").

values. Figure S3 shows that not much change in the steady states of species occurs when the parameters are varied, i.e., there is a constant change of 0.04 μM in PLS concentrations between the high and low steady-state values. Fig. 6 *C* shows the percent bistability for individual parameters when the $\pm 20\%$ (*black bars*) and $\pm 50\%$ (*gray bars*) parameter variations are compared. The parameters of production and degradation seem to influence bistability more so than other parameters, as the percent bistability decreases three-to fourfold when these parameters are varied.

DISCUSSION

In this work we used computational methods to analyze a system of UPA-mediated PLS activation. PLS is secreted as an inactive precursor and is activated by UPA as part of a positive feedback loop. Biological intuition suggests the existence of a system behavior in which both proteases are off, and another configuration of the system with both proteases strongly activated; however, the transitions and dynamic properties require quantitative analysis.

We built two computational models of the system. The first is an empirical representation of cooperativity in the form of a Hill coefficient for the kinetics of PLS (Fig. 2). The Hill coefficient could account for a wide range of simultaneous substrates with different affinities. The second computational model (Fig. 4) shows explicit substrate competition for a single anonymous competing substrate with

hypothetical affinity. Using this pair of models gives us insight into a global effect that includes a vast number of PLS substrates in a true biological system.

Cooperativity and positive feedback are accepted preconditions for the occurrence of bistability and hysteresis in a system (18,35). Lijnen et al. (33) remarked on the existence of positive feedback between PLS and UPA, and we used modeling and experiments to test whether cooperativity and bistability are also present. Model dynamics for a protease system require degradation and production because the constituent reactions are irreversible cleavage effects. Because a system with cleavage enzymatic reactions alone would inevitably tend toward a state of cleavage, synthesis of precursor proteins is required for the existence of any nontrivial equilibrium. Therefore, in the parallel experiments, we introduced exogenous uncleaved proteins at small constant rates to mimic continuous processes in vivo.

When different initial conditions (different initial activation levels of PLS) were used for the dose response to scUPA, we observed experimentally that the system could exhibit two different steady states, and hysteresis was verified. In our cell-free assay of PLS activation with different doses of UPA, we observed a sigmoidal activation response in the presence of the high-affinity S2251 chromogenic reagent for measuring PLS activity. S2251 is a substrate for PLS, and it can be presumed to occupy the active site, in competition with UPA. Competition between substrates was recently found to create cooperativity as an emergent

property of a system (25) even in the absence of allosteric cooperativity. Our experiments validate that a small change in scUPA concentration can indeed cause large absolute changes in PLS activity, with an empirical behavior of cooperativity and ultrasensitivity in the system. The PLS concentrations that show bistability in simulations (0.03–0.05 μM) would be reasonable in vivo because the total pool of PLS plus PLG was previously measured to be 0.5–2 μM (37–40). The level of scUPA needed to cause a state transition in simulations (0.7μM) is significantly above the empirical range of 0.1 nM to 0.1 μM measured for total urokinase (tcUPA plus scUPA) (41–44). Many factors could be responsible for the difference between simulated and measured urokinase values, including the greater activity of tcUPA compared with scUPA, different tissue types, and different measurement methods.

Using a Hill coefficient ci to capture various possible sources of cooperativity, we analyzed the contributions of cooperativity and positive feedback to creating bistability (Fig. 3). For example, increasing the feedback strength in the model by increasing the $keff_{pos}$ parameter caused an increased area of bistability. Of interest, increasing the $keff_{pos}$ parameter also requires an increase in the ci cooperativity parameter to maintain bistability.

The robustness analysis showed that bistability was robust to a significant range of parameter perturbations but sensitive to the production, degradation, and binding rate of the competing substrate X. Certainly the sensitivity to substrate X affinity is understandable, because a low-affinity substrate would not sequester PLS away from scUPA. The turnover of substrate X may initially seem far removed from the essence of UPA-PLS activation, but this turnover is important for determining how strong the PLS activity must be before PLS can escape the suppressive effects of sequestration, either through abundance of the PLS (outnumbering the substrate X stoichiometrically) or through catalytic efficiency (consuming the substrate X faster than it gets produced). The synthesis and degradation of substrate X regulate the threshold level at which PLS becomes cooperative because they determine the initial abundance of X and the rate at which enzymatic consumption of X is replenished.

Because the inclusion of competing substrates made the system more cooperative, it is possible that many competing substrates in a physiological context would reinforce the PLS cooperativity rather than dilute it. It is difficult to discuss steady states in a physiological context; however, certain stable and self-perpetuating modes of behavior in vivo are analogous to stable steady states. Ultrasensitive transitions between self-perpetuating modes of behavior would be in vivo analogs of bistability. Our discovery that PLS and UPA can be bistable could have important ramifications for the systems in which they participate, including angiogenesis, tumor metastasis, wound healing, and fibrosis. In other bistable signaling pathways, such as apo-

ptosis or cell cycle control, bistability permits a variety of input stimuli to be integrated into a single coordinated decision (18,45). It is interesting to speculate that the bistability of PLS and UPA might facilitate the switch-like decision of angiogenesis (46). The process of growing new blood vessels is tightly regulated by a variety of factors and occurs through an unknown switch-like decision. Because UPA and PLS are involved in various aspects of angiogenesis, such as activation of pro-angiogenic growth factors and increased degradation of interstitial matrix, these proteins are well positioned to play a coordinating role in the decisions of angiogenesis (46,47).

A bistable switch for UPA-PLS would also be useful for regulating the tight balance between inflammation and remodeling, which is needed for proper wound healing (4). The proposed switch might also have implications for healthy cell migration and pathological cell invasion, because cell motility involves coordination of proteases and other extracellular factors to remodel the ECM. PLS and UPA can act directly on the ECM (47), and also indirectly by activating many members of the canonical ECM-regulating family, the MMPs. Finally, it is important to note that bistability implies an important negative consequence, namely, that UPA and PLS would be relatively insensitive to perturbations when they are not near the ultrasensitive threshold. This negative insight may be helpful for understanding why the wound-healing response fails to switch off in fibroproliferative diseases. The bistability of the UPA/PLS subsystem may have far-reaching consequences that should be investigated in future work.

SUPPORTING MATERIAL

REFERENCES

1. Carmeliet, P., and D. Collen. 1995. Role of the plasminogen/plasmin system in thrombosis, hemostasis, restenosis and atherosclerosis evaluation in transgenic animals. *Trends Cardiovasc. Med.* 5:117–122.

2. Thompson, W. D., C. M. Stirk, …, E. B. Smith. 1996. Plasmin, fibrin degradation and angiogenesis. *Nat. Med.* 2:493.

3. Toriseva, M., and V. M. Kähäri. 2009. Proteinases in cutaneous wound healing. *Cell. Mol. Life Sci.* 66:203–224.

4. Zhang, W., L. Tucker-Kellogg, …, H. Yu. 2010. Cell-delivery therapeutics for liver regeneration. *Adv. Drug Deliv. Rev.* 62:814–826.

5. Rakic, J. M., C. Maillard, …, A. Noël. 2003. Role of plasminogen activator-plasmin system in tumor angiogenesis. *Cell. Mol. Life Sci.* 60:463–473.

6. Lijnen, H. R. 2001. Plasmin and matrix metalloproteinases in vascular remodeling. *Thromb. Haemost.* 86:324–333.

7. Ramos-DeSimone, N., E. Hahn-Dantona, …, J. P. Quigley. 1999. Activation of matrix metalloproteinase-9 (MMP-9) via a converging plasmin/stromelysin-1 cascade enhances tumor cell invasion. *J. Biol. Chem.* 274:13066–13076.

8. Hawinkels, L. J., K. Zuidwijk, …, C. F. Sier. 2008. VEGF release by MMP-9 mediated heparan sulphate cleavage induces colorectal cancer angiogenesis. *Eur. J. Cancer.* 44:1904–1913.

9. Shanmukhappa, K., U. Matte, …, J. A. Bezerra. 2009. Plasmin-mediated proteolysis is required for hepatocyte growth factor activation during liver repair. *J. Biol. Chem.* 284:12917–12923.

10. Lyons, R. M., L. E. Gentry, …, H. L. Moses. 1990. Mechanism of activation of latent recombinant transforming growth factor β 1 by plasmin. *J. Cell Biol.* 110:1361–1367.

11. Li, W. Y., S. S. Chong, …, T. L. Tuan. 2003. Plasminogen activator/plasmin system: a major player in wound healing? *Wound Repair Regen.* 11:239–247.

12. Anonick, P. K., B. Wolf, and S. L. Gonias. 1990. Regulation of plasmin, miniplasmin, and streptokinase-plasmin complex by α2-antiplasmin, α2-macroglobulin, and antithrombin III in the presence of heparin. *Thromb. Res.* 59:449–462.

13. Chen, C., J. Cui, …, P. Shen. 2007. Modeling of the role of a Bax-activation switch in the mitochondrial apoptosis decision. *Biophys. J.* 92:4304–4315.

14. Cui, J., C. Chen, …, P. Shen. 2008. Two independent positive feedbacks and bistability in the Bcl-2 apoptotic switch. *PLoS ONE.* 3:e1469.

15. Hahn-Dantona, E., N. Ramos-DeSimone, …, J. P. Quigley. 1999. Activation of proMMP-9 by a plasmin/MMP-3 cascade in a tumor cell model. Regulation by tissue inhibitors of metalloproteinases. *Ann. N. Y. Acad. Sci.* 878:372–387.

16. Schenone, M., B. C. Furie, and B. Furie. 2004. The blood coagulation cascade. *Curr. Opin. Hematol.* 11:272–277.

17. Angeli, D. 2006. New analysis technique for multistability detection. *Syst. Biol. (Stevenage).* 153:61–69.

18. Bhalla, U. S., and R. Iyengar. 1999. Emergent properties of networks of biological signaling pathways. *Science.* 283:381–387.

19. Huang, C. Y., and J. E. Ferrell, Jr. 1996. Ultrasensitivity in the mitogen-activated protein kinase cascade. *Proc. Natl. Acad. Sci. USA.* 93:10078–10083.

20. Markevich, N. I., J. B. Hoek, and B. N. Kholodenko. 2004. Signaling switches and bistability arising from multisite phosphorylation in protein kinase cascades. *J. Cell Biol.* 164:353–359.

21. Bagowski, C. P., and J. E. Ferrell, Jr. 2001. Bistability in the JNK cascade. *Curr. Biol.* 11:1176–1182.

22. Aldridge, B. B., J. M. Burke, …, P. K. Sorger. 2006. Physicochemical modelling of cell signalling pathways. *Nat. Cell Biol.* 8:1195–1203.

23. Novak, B., J. J. Tyson, …, A. Csikasz-Nagy. 2007. Irreversible cell-cycle transitions are due to systems-level feedback. *Nat. Cell Biol.* 9:724–728.

24. Eissing, T., S. Waldherr, …, E. Bullinger. 2007. Steady state and (bi-) stability evaluation of simple protease signalling networks. *Biosystems.* 90:591–601.

25. Kim, S. Y., and J. E. Ferrell, Jr. 2007. Substrate competition as a source of ultrasensitivity in the inactivation of Wee1. *Cell.* 128:1133–1145.

26. Lüthi, A. U., and S. J. Martin. 2007. The CASBAH: a searchable database of caspase substrates. *Cell Death Differ.* 14:641–650.

27. Stennicke, H. R., and G. S. Salvesen. 1999. Catalytic properties of the caspases. *Cell Death Differ.* 6:1054–1059.

28. Chen, C., J. Cui, …, P. Shen. 2007. Robustness analysis identifies the plausible model of the Bcl-2 apoptotic switch. *FEBS Lett.* 581:5143–5150.

29. Collen, D., C. Zamarron, …, M. Hoylaerts. 1986. Activation of plasminogen by pro-urokinase. II. Kinetics. *J. Biol. Chem.* 261:1259–1266.

30. Pannell, R., and V. Gurewich. 1987. Activation of plasminogen by single-chain urokinase or by two-chain urokinase—a demonstration that single-chain urokinase has a low catalytic activity (pro-urokinase). *Blood.* 69:22–26.

31. Ellis, V., M. F. Scully, and V. V. Kakkar. 1987. Plasminogen activation by single-chain urokinase in functional isolation. A kinetic study. *J. Biol. Chem.* 262:14998–15003.

32. Lucas, M. A., D. L. Straight, …, P. A. McKee. 1983. The effects of fibrinogen and its cleavage products on the kinetics of plasminogen activation by urokinase and subsequent plasmin activity. *J. Biol. Chem.* 258:12171–12177.

33. Lijnen, H. R., B. Van Hoef, …, D. Collen. 1989. The mechanism of plasminogen activation and fibrin dissolution by single chain urokinase-type plasminogen activator in a plasma milieu in vitro. *Blood.* 73:1864–1872.

34. Blüthgen, N., S. Legewie, …, B. Kholodenko. 2007. Mechanisms generating ultrasensitivity, bistability, and oscillations in signal transduction. *In* Introduction to Systems Biology. S. Choi, editor. Humana Press, Totowa, NJ. 282–299.

35. Ferrell, Jr., J. E. 2002. Self-perpetuating states in signal transduction: positive feedback, double-negative feedback and bistability. *Curr. Opin. Cell Biol.* 14:140–148.

36. Reinhart, G. D., and H. A. Lardy. 1980. Rat liver phosphofructokinase: kinetic activity under near-physiological conditions. *Biochemistry.* 19:1477–1484.

37. Robbins, K. C., and L. Summaria. 1970. Human plasminogen and plasmin. *In* Methods in Enzymology. J. N. Abelson and M. I. Simon, editors. Academic Press, New York. 184–199.

38. Lijnen, H. R., and D. Collen. 1982. Interaction of plasminogen activators and inhibitors with plasminogen and fibrin. *Semin. Thromb. Hemost.* 8:2–10.

39. Collen, D., G. Tytgat, …, P. Wallén. 1972. Metabolism of plasminogen in healthy subjects: effect of tranexamic acid. *J. Clin. Invest.* 51:1310–1318.

40. Soulat, T., S. Loyau, …, E. Anglés-Cano. 1999. Evidence that modifications of Lp(a) in vivo inhibit plasmin formation on fibrin—a study with individual plasmas presenting natural variations of Lp(a). *Thromb. Haemost.* 82:121–127.

41. Shakespeare, M., and P. Wolf. 1979. The demonstration of urokinase antigen in whole blood. *Thromb. Res.* 14:825–835.

42. Saito, K., M. Nagashima, …, A. Takada. 1990. The concentration of tissue plasminogen activator and urokinase in plasma and tissues of patients with ovarian and uterine tumors. *Thromb. Res.* 58:355–366.

43. Koelbl, H., J. C. Kirchheimer, …, B. R. Binder. 1988. Increased plasma levels of urokinase-type plasminogen activator with endometrial and cervical cancer. *Obstet. Gynecol.* 72:252–256.

44. Wankiewicz, A., I. Iwan-Zietek, …, Z. Gwieździński. 2002. Selected parameters of fibrinolysis system in patients with dermatitis herpetiformis. *Med. Sci. Monit.* 8:CR189–CR192.

45. Bagci, E. Z., Y. Vodovotz, …, I. Bahar. 2006. Bistability in apoptosis: roles of bax, bcl-2, and mitochondrial permeability transition pores. *Biophys. J.* 90:1546–1559.

46. Ribatti, D., B. Nico, …, A. Vacca. 2007. The history of the angiogenic switch concept. *Leukemia.* 21:44–52.

47. van Hinsbergh, V. W., M. A. Engelse, and P. H. Quax. 2006. Pericellular proteases in angiogenesis and vasculogenesis. *Arterioscler. Thromb. Vasc. Biol.* 26:716–728.

48. Wang, M., D. Zhao, …, E. G. Lakatta. 2006. Matrix metalloproteinase 2 activation of transforming growth factor-β1 (TGF-β1) and

TGF-β1-type II receptor signaling within the aged arterial wall. *Arterioscler. Thromb. Vasc. Biol.* 26:1503–1509.

49. Eissing, T., H. Conzelmann, …, P. Scheurich. 2004. Bistability analyses of a caspase activation model for receptor-induced apoptosis. *J. Biol. Chem.* 279:36892–36897.

50. Travis, J., and G. S. Salvesen. 1983. Human plasma proteinase inhibitors. *Annu. Rev. Biochem.* 52:655–709.

51. Köhler, M., S. Sen, …, K. Hollemeyer. 1991. Half-life of single-chain urokinase-type plasminogen activator (scu-PA) and two-chain urokinase-type plasminogen activator (tcu-PA) in patients with acute myocardial infarction. *Thromb. Res.* 62:75–81.

52. Legewie, S., N. Blüthgen, and H. Herzel. 2006. Mathematical modeling identifies inhibitors of apoptosis as mediators of positive feedback and bistability. *PLOS Comput. Biol.* 2:e120.